# THERMAL RADIATION DISTRIBUTION ON SAMPLES TESTED IN CONE AND CYLINDER CALORIMETERS

**Marcos Jorge Alves Gemaque, mgemaque@hotmail.com**
*Instituto de Estudos Avançados, CTA, São José dos Campos, SP*

**Fernando de Souza Costa, fernando@lcp.inpe.br**
*Laboratório Associado de Combustão e Propulsão, INPE, Cachoeira Paulista, SP*

***Abstract.*** *Cone and cylinder calorimeters are devices used to determine the characteristics of pyrolysis, ignition and combustion of slabs and cylinders of solid materials, such as polymers, wood and other cellulosic materials. The objective of this work was to determine the theoretical distribution of thermal radiation on samples under a prescribed heating rate in cone and cylinder calorimeters, and to study the effects of variations of position and size of the samples. Expressions for the radiation form factors are derived and calculated by MATLAB codes. The results indicate that the total amount and the distribution of thermal radiation can be significantly affected by size differences or by positioning errors of the samples in the calorimeters. It is verified that cone calorimeters are more sensitive to variations in sample size and positioning errors than cylinder calorimeters.*

***Keywords****: Cone calorimeter, cylindrical calorimeter, radiation form factor, position error, size effects*

## 1. INTRODUCTION

Cone and cylinder calorimeters are used to determine the characteristics of pyrolysis, ignition and burning of slabs and cylinders of solid materials, such the wood, celullosic materials and polymers. These calorimeters allow obtaining the heat release rates, fuel consumption rates, instantaneous mass, effective heat of combustion, visible smoke release, emissions of warm samples under predefined flows of heat, with or without external ignition, and other characteristics.

Tests in cone calorimeters are referenced in the ASTM E1354-03 "Standard Test Method for Determination of Heat and Visible Smoke Release Rates for Materials and Products Using an Oxygen Consumption Calorimeter". The heat release rates of slabs 100×100×50 $mm^3$ is determined by measurements of the oxygen concentration in the exhaustion gases. The cylinder calorimeter was developed by Castro and Costa (2005) for the characterization of the burning of wood cylinders with 100 mm of height and 10 to 30 mm of diameter, with different percentages of humidity.

An important point to be considered is the relation between volumes of the samples used in the calorimeters. The volumes of the slabs tested in the conical calorimeter are 7 to 28 times the volumes of the cylinders tested in the cylindrical calorimeter. the consequence, the operation cost of the cylinder calorimeter can be significantly inferior to the conical calorimeter, considering the sample mass, the power input required and the time needed for burning the samples.

Figure 1 shows photos of the conical and cylindrical calorimeters in operation.

Figure 2 shows a random survey of publications related to cone calorimeters. About 60 articles were selected in international scientific journals, including Fire Technology Journal, Combustion and Flame, Polymer Degradation and Stability Journal, amongst others. The articles were separated in different study categories.

This short survey indicates that most demands in the use of calorimeters concentrate in the determination of heat release rates and in the determination of flammability properties of materials. An example is the work developed by Janowska et al. (2007) that presented results concerning the thermal stability of rubber vulcanized with butadiene and acrylonitrile, with varying amounts of silica containing bromine and iodine. A considerable reduction in rubber flammability was found by increasing the modified silica content. Dennis Price et al. (2005) made studies of the characterization of fire retardants, evaluating the inhibition of polystyrene burning by incorporation of phosphor compounds. A practical application is presented in the work of Elliot and Whiteney (1998) which tested four commercial wire types with a protocol that presented a good repeatability. The results demonstrated a negative impact of the insulation with a clorinated polyethylene base, containing antimony trioxide, on the production of smoke and CO, compared with an equivalent system without halogen. A numerical study about the operation of calorimeters was presented by Hostikka and Axelsson (2003). They developed CFD codes to model the turbulent flames on samples in a cone calorimeter, considering the radiation from the flame and the calorimeter, the convection and the presence of soot. Their computational results are useful to extend the applications of cone calorimeters to the field of fire safety engineering, where more accurate data of pyrolysis rates in function of the heat input are necessary.

An example of study about celullosic materials using cone and cylinder calorimeters is given by Castro and Costa (2007) that determined the evolution of temperatures and propagation rates of drying, pyrolysis and smoldering fronts in wood samples. They verified a significant reduction of the reaction rates in wood cylinders caused by the increase of the humidity. The orientation of wood fibers had in the significant effect in the reaction rates of slabs heated in a cone calorimeter. It is observed that the presence of the flame produces an important increase in the increase rate of the

temperature and in the pyrolysis of the wood. The celullosic samples present a heterogeneous and anisotropic structure that affects the burning characteristics.

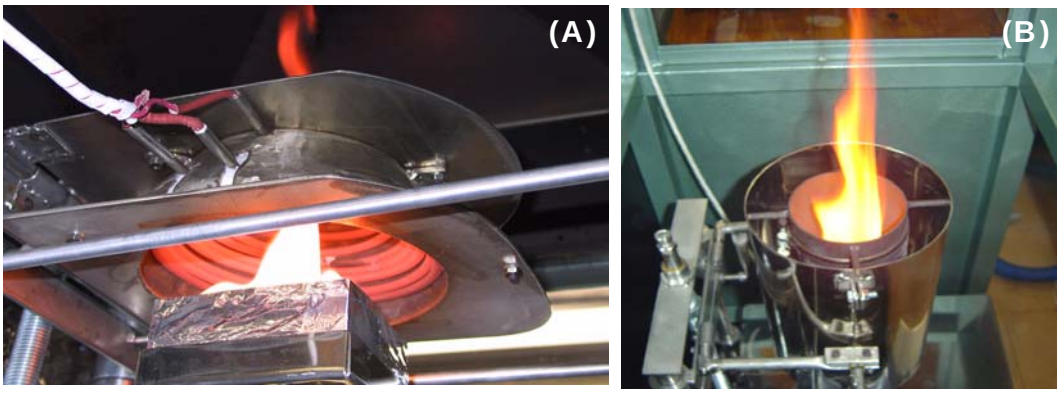


Figure 1. (A) Cone calorimeter; (B) Cylinder calorimeter.

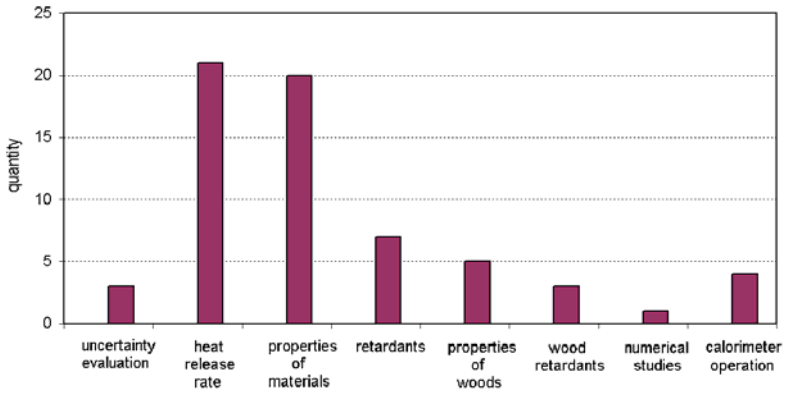


Figure 2 – Number of publications in different categories related to cone calorimeters.

The objective of this work is to calculate the distribution of thermal radiation on slabs and cylinders heated inside cone and cylinder calorimeters, respectively. It is made analysis of the effects of variations in position and sample size on the incident heat flow distribution. A numerical code, written in MATLAB language, is used to calculate the radiation form factors between the calorimeters and the surfaces of the samples. The results can be useful for comparison with experimental results and to define the operation envelopes of the calorimeters.

## 2. ANALYSIS

This work focuses on the heat radiation transfer process from cone and cylinder calorimeters to their samples. It should be noted that conduction and convection heat transfer processes also occur and can affect the temperature distribution. In the next sections concepts about radiation heat transfer are presented and used to determine the fractions of the energy radiated from the calorimeters that reach the surface of samples of different sizes and positionings.

### 2.1. Thermal Radiation and Form Factor

Thermal radiation is the electromagnetic radiation emitted by a body the function of its temperature. When two bodies, 1 and 2, exchange heat by radiation, the net heat transfer is proportional to the difference between the fourth powers of the thermodynamic temperatures of the surfaces of the bodies. Thus, $\dot{q} = \varepsilon\sigma F_{1-2} A_1 (T_1^4 - T_2^4)$, where $\varepsilon$ is the emissivity of body 1, $\sigma = 5{,}669\times10^{-8}$ W/m$^2$K$^4$ is the Stefan-Boltzmann constant, $A_1$ is the radiant area of body 1, $T_1$ and $T_2$ are, respectively, the temperatures of bodies 1 and 2, and the factor $F_{1\text{-}2}$ indicates the fraction of the energy irradiated by the body 1 surface that reaches the body 2 surface.

The form factor $F_{1\text{-}2}$ depends on the relative position and orientation of the surface areas of the bodies exchanging heat. Therefore, a change in the dimensions of the surface areas or in the relative position of the bodies will cause a variation of the form factor and, consequently, modify the fraction of thermal radiation energy that leaves one body and reaches the other. Figure 2 shows two surfaces, $A_1$ and $A_2$, with arbitrary relative orientation, exchanging heat by radiation.

Before determination of the form factor $F_{2\text{-}1}$ between surfaces $A_1$ and $A_2$, two differential elements of area, $dA_1$ and $dA_2$, are first considered, as shown in Figure 3. The angles $\theta_1$ and $\theta_2$ are measured between the normal vectors to the area elements and the segment of length $S$ connecting the centers of the area elements.

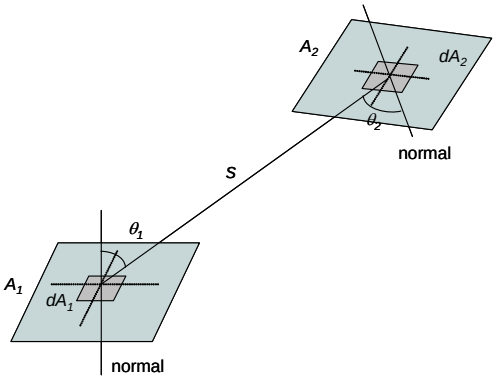


Figure 3. Two surfaces, $A_1$ and $A_2$, exchanging heat by radiation, with arbitrary positions and orientations.

The form factor between two differential elements $dA_1$ and $dA_2$ (Siegel and Howell, 1992) is given by:

$$dF_{d1-d2} = \frac{\cos\theta_1 \cos\theta_2}{\pi S^2} dA_2 \tag{1}$$

Consequently, it can be easily verified that $dA_1 dF_{d1-d2} = dA_2 dF_{d2-d1}$. To get the form factor from an area element $dA_1$ to an area $A_2$, Eq. (1) is integrated, yielding:

$$dF_{d1-2} = \int_{A_2} \frac{\cos\theta_1 \cos\theta_2}{\pi S^2} dA_2 \tag{2}$$

It can be also verified that $dA_1 dF_{d1-2} = A_2 dF_{2-d1}$. Integrating Eq. (2) through area $A_1$, it gives the form factor between surfaces $A_1$ and $A_2$:

$$F_{1-2} = \frac{1}{A_1} \int_{A_1} \int_{A_2} \frac{\cos\theta_1 \cos\theta_2}{\pi S^2} dA_2 dA_1 \tag{3}$$

Similarly to the other cases, it can be verified a reciprocity relation, $A_1 F_{1-2} = A_2 F_{2-1}$.

In the next section, the previous equations are used to calculate the form factors between the surface area elements or the complete exposed surfaces of the samples and the calorimeters.

### 2.2. Form factor between a cone calorimeter and the exposed surface of a square slab

Figure 4 shows a scheme of the cone calorimeter and the exposed surface of the sample, a square of side $l$ located at a distance $h_2$ from the base of the cone calorimeter (cone frustum). The axis of the cone frustum is perpendicular to the square and passes by its center. The base circle of the cone frustum has radius $R_2$ and the top circle has radius $R_4$ and is located at a distance $h_4$ from the square.

It is required to calculate the form factor between the internal surface of the cone frustum, $A_3$, and the square, $A_1$. First, the inverse problem is considered, i.e., it is calculated the fraction of the radiation that, coming from the square, would reach the cone frustum. It can be verified that $F_{1-3} = F_{1-2} - F_{1-4}$, and using the reciprocity relation $A_1 F_{1-3} = A_3 F_{3-1}$, it gives:

$$F_{3-1} = \frac{A_1}{A_3}\left(F_{1-2} - F_{1-4}\right) \tag{4}$$

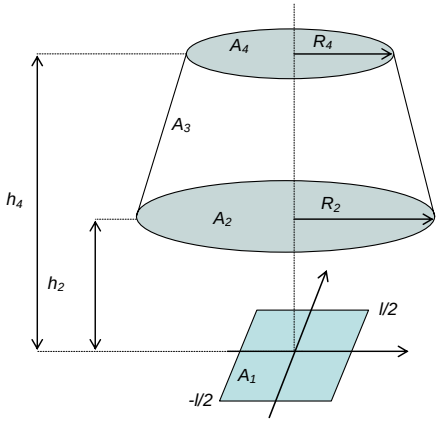


Figure 4. Scheme of a cone calorimeter and the exposed surface of a sample (square slab).

The problem now is to determine the form factors between the square of side $l$ and the circles with radii $R_2$ and $R_4$. Figure 5 shows an area element of the square radiating to an area element of the circle located at a distance $h$ of the square plane. The area element of the circle belongs to a ring with infinitesimal thickness $dr$.

From Fig. 5, it can is seen that $\theta_1 = \theta_2$. Therefore, $\cos\theta_1 = \cos\theta_2$, with $\cos\theta_2 = h/s$. Using these results and Eq. (1), it follows that

$$F_{d1-d2} = \frac{\cos\theta_1 \cos\theta_2}{\pi s^2} dA_2 = \frac{\cos\theta_2^{\,2}}{\pi s^2} dA_2 = \frac{h^2}{\pi s^4} dA_2$$

Substituting $dA_2 = r\, d\phi\, dr$ in the last equation and considering the Eq. (2), it yields

$$F_{d1-2} = \int_{r=0}^{R} \int_{\phi=0}^{2\pi} \frac{h^2}{\pi s^4} r\, d\phi\, dr$$

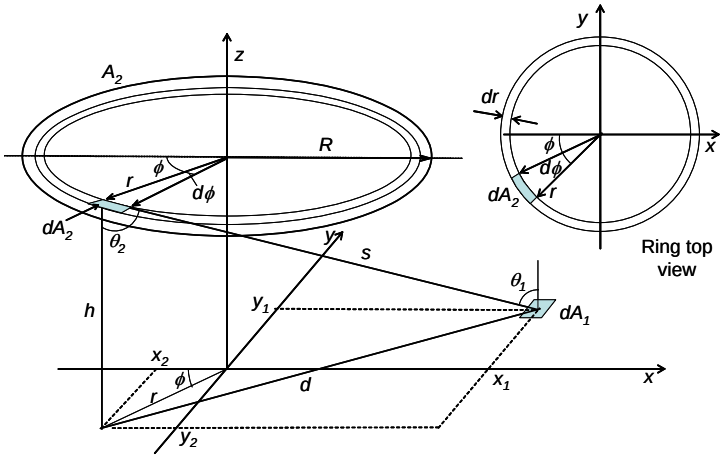


Figure 5. Form factor between an area element $dA_1$ of a square and an area element $dA_2$ of a circle.

From Fig. (5), $S^2 = h^2 + d^2 = h^2 + (x_2 - x_1)^2 + (y_2 - y_1)^2$, $x_2 = r\cos\phi$ and $y_2 = rsen\phi$. Therefore, $S^2 = h^2 + d^2 = h^2 + (r\cos\phi - x_1)^2 + (rsen\phi - y_1)^2$ and, then

$$F_{d1-2} = \int_{r=0}^{R} \int_{\phi=0}^{2\pi} \frac{h^2 r}{\pi\left[h^2 + (r\cos\phi - x_1)^2 + (rsen\phi - y_1)^2\right]^2} d\phi\, dr$$

Using Eq. (3) and considering the geometry,

$$F_{1-2} = \frac{4}{A_1} \int_{x_1=0}^{l/2} \int_{y_1=0}^{l/2} \int_{r=0}^{R_2} \int_{\phi=0}^{2\pi} \frac{h_2^2 r}{\pi\left[h_2^2 + (r\cos\phi - x_1)^2 + (rsen\phi - y_1)^2\right]^2} d\phi\, dr\, dx_1\, dy_1 \qquad (5)$$

Analogously,

$$F_{1-4} = \frac{4}{A_1}\int_{x_1=0}^{l/2}\int_{y_1=0}^{l/2}\int_{r=0}^{R_4}\int_{\phi=0}^{2\pi}\frac{h_4^2 r}{\pi\left[h_4^2+\left(r\cos\phi-x_1\right)^2+\left(rsen\phi-y_1\right)^2\right]^2}d\phi\, dr\, dx_1\, dy_1 \tag{6}$$

Substituting Eqs. (5) and (6) into Eq. (4), it yields the form factor between the cone frustum, $A_3$, and the square, $A_1$:

$$F_{3-1} = \frac{4}{A_3}\left[\int_{x_1=0}^{l/2}\int_{y_1=0}^{l/2}\int_{r=0}^{R_2}\int_{\phi=0}^{2\pi}\frac{h_2^2 r}{\pi\left[h_2^2+\left(r\cos\phi-x_1\right)^2+\left(rsen\phi-y_1\right)^2\right]^2}d\phi dr dx_1 dy_1 + \right.$$
$$\left. -\int_{x_1=0}^{l/2}\int_{y_1=0}^{l/2}\int_{r=0}^{R_4}\int_{\phi=0}^{2\pi}\frac{h_4^2 r}{\pi\left[h_4^2+\left(r\cos\phi-x_1\right)^2+\left(rsen\phi-y_1\right)^2\right]^2}d\phi dr dx_1 dy_1\right] \tag{7}$$

### 2.3. Form factor between a cylinder calorimeter and a coaxial cylinder

Figure 6 shows a scheme of a cylinder calorimeter (external cylinder) and the exposed surface (side and top) of the sample (internal cylinder). The calorimeter has a height $H$, radius $r_2$ and side area $A_2$. The sample has side area $A_1$, radius $r_1$ and area of the top circle $A_{1'}$. The side area of the calorimeter above the top of the sample is designated $A_{2'}$.

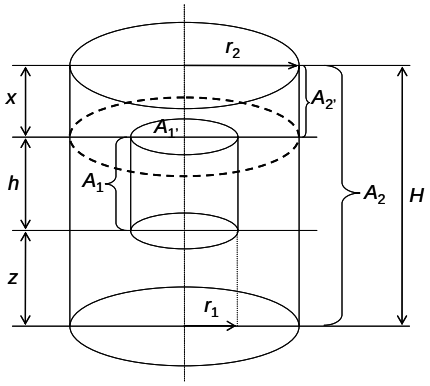


Figure 6. Scheme of a cylinder calorimeter and a cylindrical sample.

The form factor between the internal surface of the external cylinder, with area $A_2$, and the side of the internal cylinder, with area $A_1$, is given by following equation (Rea, 1975 ):

$$F_{2-1} = \frac{A_1}{A_2}\left[1+\frac{X}{L}F_X+\frac{Z}{L}F_Z-\left\{\frac{L+X}{L}\right\}F_{L+X}-\left\{\frac{L+Z}{L}\right\}F_{L+Z}\right] \tag{8}$$

where

$$F_\xi = \frac{D_\xi}{8R\xi}+\frac{1}{2\pi}\left\{\cos^{-1}\frac{C_\xi}{D_\xi}-\frac{1}{2\xi}\left[\frac{\left(C_\xi+2\right)^2}{R^2}-4\right]^{1/2}\cos^{-1}\frac{C_\xi R}{D_\xi}-\frac{C_\xi}{2R\xi}sen^{-1}R\right\}$$

$C_\xi = \xi^2+R^2-1$ ; $D_\xi = \xi^2-R^2+1$; $X = x/r_2$ ; $Z = z/r_2$ ; $L = h/r_2$ and $R = r_1/r_2$ .

The form factor between surfaces $A_{2'}$ and $A_{1'}$ is obtained from results obtained by Buschman and Pittmann (1961):

$$F_{2'-1'} = \frac{1}{4RH}\left[\left(X_2-X_1\right)-\left(X_2-4R^2\right)^{1/2}+\left(X_1-4R^2\right)^{1/2}\right] \tag{9}$$

where $R = r_2/r_1$ ; $H = x/r_1$ ; $X_1 = H^2+R^2+1$ and $X_2 = R^2+1$

The sum of Eqs. (8) and (9) gives the fraction of the thermal radiation coming from the cylinder calorimeter that reaches the sample, i.e., $F_{(2-1)_T} = F_{2-1} + F_{2'-1'}$, where the subscript $T$ designates total.

## 3. RESULTS

Two MATLAB codes were written to solve Eqs. (7), (8) and (9) and calculate the radiation form factors between the cone and cylinder calorimeters and their respective samples (Adade, 2001).

Figure 7 shows the results obtained for the distribution of thermal radiation per unity area of the exposed surface of a slab, as a function of the distance, $h_2$, from the slab to the base circle of the cone calorimeter. The radiation distribution was calculated for $h_2$ = 10, 20, 30 and 40 *mm*. Because of the problem symmetry, the plots show only a quarter of the slab exposed surface. Each quadrant was divided in 50 × 50 differential elements.

Figure 8 shows the form factor per unity area along the diagonal of the slab surface.

Table 1 shows the form factors between the cone calorimeter and the total exposed surface of the sample, as function of the distance $h_2$, for $l$ = 100 *mm*, and as function of the side $l$ of the square slab, for $h_2$ = 10 *mm*.

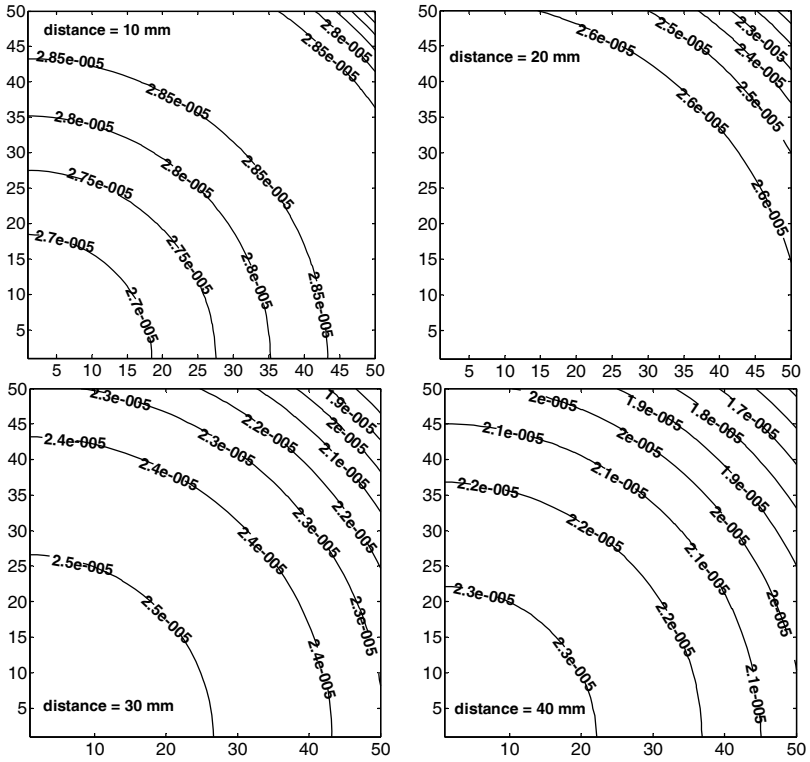


Figure 7. Effects of distance, $h_2$ (*mm*), from the sample surface to the base of a cone calorimeter, on thermal radiation distribution per unity area ($mm^2$) of the sample surface.

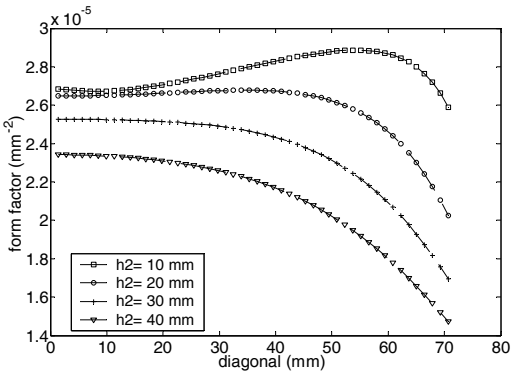


Figure 8. Form factor per unity area ($mm^2$) along the diagonal of the exposed surface of a square slab.

Table 1. Effects of the distance $h_2$, from the exposed surface of a slab to the base of the cone calorimeter, and effects of the side $l$ of a square slab on the total form factor between the cone calorimeter and the slab surface.

| $h_2$ (*mm*) | Total form factor | variation in relation to $h_2$ = 10 *mm* (%) | $l$ (*mm*) | Total form factor | variation in relation to $l$ = 100 *mm* (%) |
|---|---|---|---|---|---|
| 10 | 0.2808 | 0.00 | 80 | 0.1777 | –36.71 |
| 20 | 0.2628 | –6.41 | 90 | 0.2265 | –19.35 |
| 30 | 0.2383 | –15.15 | 100 | 0.2808 | 0.00 |
| 40 | 0.2127 | –24.26 | 110 | 0.3393 | 20.84 |

In the case of the cylinder calorimeter it was considered, initially, the effect of the variation of the sample radius, $r_1$, on the radiation distribution on the side and top surfaces of the sample, as depicted in Figures 9a and 9b, respectively.

For the analysis of the total form factor between the cylinder calorimeter and a cylindrical sample, it was considered the variation of the sample height ($h$) and the variation of the distance ($z$) from the calorimeter base to the sample base.

Figure 10a shows the total form factor between the cylinder calorimeter and the surface of the sample as function of the height, $h$, and of the radius, $r_1$, of a cylinder positioned in $z$ = 75 *mm*.

Table 2 shows the form factors, $F_{(2-1)_T}$, and their percent variations, $\Delta$, between the calorimeter and the surface of the sample, as function of height, $h$, and radius, $r_1$, of the cylindrical sample. The variations are relative to the form factor of a cylinder with $h$ = 100 *mm*, positioned in $z$ = 75 *mm*.

Figure 10b shows the form factor between the cylinder calorimeter and the sample surface as function of position, $z$, and radius, $r_1$, of a sample with $h$ = 100 *mm*.

Table 3 shows the form factors, $F_{(2-1)_T}$, and their percent variations, $\Delta$, between the calorimeter and the sample surface, the function of position, $z$, and radius, $r_1$. The variations are relative to the form factor of a cylinder positioned in $z$ = 75 *mm*, with $h$ = 100 *mm*.

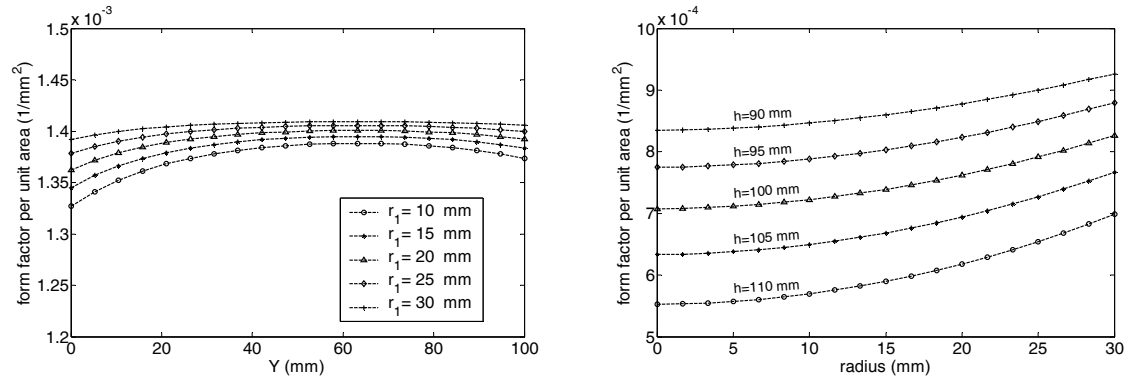


a) b)

Figure 9. a) Form factor per unity area ($mm^2$) along the side of a cylindrical sample in a cylinder calorimeter, as function of the vertical position ($y$) and radius, $r_1$, of the sample. b) Form factor per unity area ($mm^2$) along the top surface, as function of height $h$ and radius, $r_1$, of the sample.

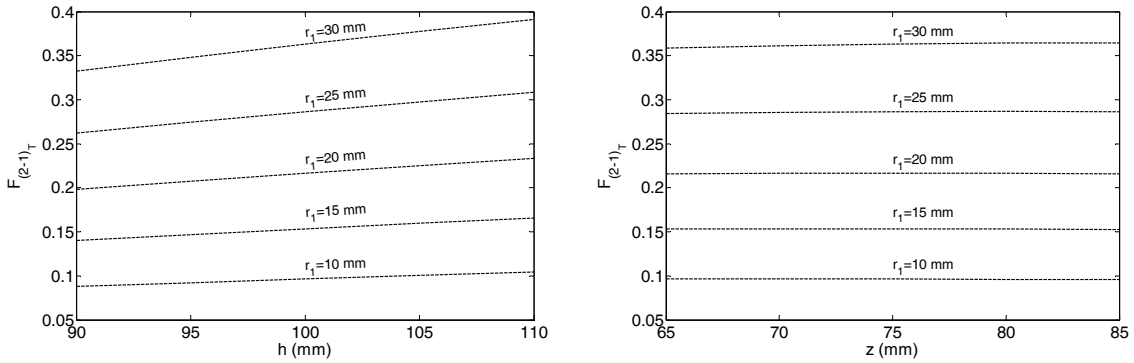


a) b)

Figure 10. a) Total form factor between a cylinder calorimeter and the sample surface as function of height, $h$, and radius, $r_1$, of a sample positioned in $z$ = 75 *mm*. b) Total form factor between the cylinder calorimeter and the sample surface as function of position, $z$, and radius, $r_1$, for cylindrical samples with $h$ = 100 *mm*.

Table 2. Total form factors, $F_{(2-1)_T}$, and their percent variations, Δ, between the cylinder calorimeter and the sample surface, as function of height, *h*, and radius, $r_1$, of the sample. The variations are relative to the form factor of a cylinder with $h$ = 100 *mm*, positioned in $z$ = 75 *mm*.

| $h$ (*mm*) | $r_1$ = 10 *mm* | | $r_1$ = 15 *mm* | | $R_1$ = 20 *mm* | | $r_1$ = 25 *mm* | | $r_1$ = 30 *mm* | |
|---|---|---|---|---|---|---|---|---|---|---|
| | $F_{(2-1)_T}$ | Δ (%) | $F_{(2-1)_T}$ | Δ (%) | $F_{(2-1)_T}$ | Δ (%) | $F_{(2-1)_T}$ | Δ (%) | $F_{(2-1)_T}$ | Δ (%) |
| 90 | 0.088 | –8.91 | 0.140 | –8.66 | 0.198 | –8.49 | 0.262 | –8.42 | 0.332 | –8.43 |
| 95 | 0.092 | –4.46 | 0.147 | –4.30 | 0.208 | –4.16 | 0.274 | –4.16 | 0.348 | –4.16 |
| 100 | 0.097 | 0.00 | 0.154 | 0.00 | 0.217 | 0.00 | 0.286 | 0.00 | 0.363 | 0.00 |
| 105 | 0.101 | 4.25 | 0.160 | 4.04 | 0.225 | 3.97 | 0.298 | 3.95 | 0.378 | 3.99 |
| 110 | 0.104 | 8.19 | 0.166 | 7.88 | 0.233 | 7.71 | 0.308 | 7.61 | 0.391 | 7.71 |

Table 3. Total form factors, $F_{(2-1)_T}$, and their percent variations, Δ, between the calorimeter and the sample surface, as function of position, $z$, and radius, $r_1$, of the sample. The variations are relative to the form factor of a cylinder located in $z$ = 75 *mm*, with $h$ = 100 *mm*.

| $z$ (*mm*) | $r_1$ = 10 *mm* | | $r_1$ = 15 *mm* | | $r_1$ = 20 *mm* | | $r_1$ = 25 *mm* | | $r_1$ = 30 *mm* | |
|---|---|---|---|---|---|---|---|---|---|---|
| | $F_{(2-1)_T}$ | Δ (%) | $F_{(2-1)_T}$ | Δ (%) | $F_{(2-1)_T}$ | Δ (%) | $F_{(2-1)_T}$ | Δ (%) | $F_{(2-1)_T}$ | Δ (%) |
| 65 | 0.0965 | 0.0000 | 0.1532 | –0.1954 | 0.2156 | –0.4617 | 0.2841 | –0.7684 | 0.3589 | –1.1295 |
| 70 | 0.0965 | 0.0000 | 0.1534 | –0.0651 | 0.2163 | –0.1385 | 0.2854 | –0.3144 | 0.3611 | –0.5234 |
| 75 | 0.0965 | 0.0000 | 0.1535 | 0.0000 | 0.2166 | 0.0000 | 0.2863 | 0.0000 | 0.3630 | 0.0000 |
| 80 | 0.0962 | –0.3109 | 0.1532 | –0.1954 | 0.2165 | –0.0462 | 0.2866 | 0.1048 | 0.3642 | 0.3306 |
| 85 | 0.0958 | –0.7254 | 0.1525 | –0.6515 | 0.2157 | –0.4155 | 0.2861 | –0.0699 | 0.3645 | 0.4132 |

## 5. DISCUSSION

It can be noted in Figs. 6 and 7 a significant reduction in the form factor or incident heat flux on the area elements of the slab exposed surface, when the distance $h_2$ increases from 10 to 40 *mm*. In the middle of the square section (sample sector), and in the boundaries, the variations are about 22 % and 45 %, respectively. The heat flow distribution is more uniform for $h_2$ = 20 *mm* than for $h_2$ = 25 *mm* which is the distance established by the ASTM E1354–03 standard.

Table 1 shows a reduction of approximately 24 % in the incident radiation when the distance from the sample to the base of the calorimeter increases from 10 to 40 *mm* and it is observed a decrease of the incident thermal radiation of about 37 % when the slab side is reduced from 100 to 80 *mm*, that is, 20 % of the length, *l*, and there is also an increase of about 40 % in the incident radiation when the slab side is increased 22 %, from 90 to 110 *mm*.

In the case of cylinder calorimeters, the form factors were determined between the cylinder calorimeter and the unity areas on the side and top of the cylindrical samples and between the cylinder calorimeter and the total sample surface.

Figure 8 shows the form factor per unity area between the cylinder calorimeter and the side of the cylindrical sample. The maximum percent variation is about 7 % in the base of the sample, 2,8 % in the central region, where occur local maximums of the form factors, and 4 % on the top of the cylinder, for sample radius $r_1$ varying from 10 *mm* to 30 *mm*.

For evaluation of the form factor per unity area of the cylinder calorimeter to the top of the sample, seen in Figure 9a, it is observed a percent increase up to 27 % from the center of the sample to the boundaries, for $h$ varying from 90 to 110 mm.

In Figure 9b it is observed an approximately linear behavior of the form factor between the cylinder calorimeter and the total sample surface. Variation of the height $h$ around 100 *mm* for several radii of the sample shows a gradient with small inclination, but increasing with larger sample radii. The gradient is 0.015 of the energy fraction / mm for $r_1$ = 10 *mm* and 0,025 of the energy fraction / mm for $r_1$= 30 *mm*.

From Table 2, the form factor variation with respect to $h$ = 100 *mm* is around 8 %, for all $r_1$ values. The variation percent values are negative for $h$ smaller than 100 *mm* and positive for $h$ larger than 100 *mm*.

In Figure 10a, it is observed also an almost linear behavior of the form factor between the cylinder calorimeter and the sample surface. Variations in position, around $z$ = 75 *mm*, for several sample radii show a less steep gradient than in the previous case, but increasing for larger sample radii.

From Table 3, the maximum variation of the form factor with respect to $z$ = 75 *mm* is about –0.7 % and +1.1%, for $r_1$ equal to 10 *mm* and 30 *mm*, respectively.

## 6. CONCLUSIONS

This work has presented the distribution of thermal radiation and the effects of variations in position and size differences on samples heated under controlled conditions inside cone and cylinder calorimeters. Expressions for the form factors between a cone frustum and a square, and between concentric cylinders of different lengths were presented.

It was verified that the cone calorimeter has a larger sensitivity to variations in sample position and size than the cylinder calorimeter. This happens because the heat flow is more concentrated at the center of the slab sample inside the cone calorimeter. There is a significant reduction in the form factor, about 24 %, when the distance $h_2$ is quadrupled and a variation of about 40 % when the slab side is increased or reduced in 20%.

The variations found in the form factors between samples and a cylinder calorimeter were relatively small when compared to the cone calorimeter. It was verified a good stability of the total form factor, $F_{(2-1)_r}$, in the cylinder calorimeter, with a larger influence of height ($h$) variations than position variations ($z$) of the cylindrical samples.

Unless it is strictly required to use a slab, the cylinder calorimeter has advantages that justify its adoption. Besides its lower sensitivity to errors in sample position and size differences, the cylinder calorimeter is easier to construct, due to its simpler geometry, and its operational cost is significantly lower, since the slabs tested in the cone calorimeter have volumes 7 to 28 times larger than the volumes of the cylinders tested in the cylinder calorimeter. Consequently, the amount of material, the power input and the operation time are smaller when the cylinder calorimeter is used.

Additional work is required to quantify the influences of the conduction and convection processes during tests in calorimeters, considering variations in sample size and position.

## 7. REFERENCES

Adade, A. F., Matlab Básico 6, São José dos Campos, CTA-ITA, 2001.

ASTM E1354–03, Standard Test Method for Heat and Visible Smoke Release Rates for Materials and Products Using an Oxygen Consumption Calorimeter, ASTM, Designation: and 1354 – 03.

Buschman, A.J.J., Pittmann, C.M., Configuration Factor for Exchange of Radiant Energy between Axisymmetrical Sections of Cylinders, Cones, and Hemispheres and their bases, NASA TN D-944, Oct., 1961.

Castro, A., Investigação Teórico-Experimental of the Combustão de Madeira, Dissertação de Mestrado em Engenharia and Tecnologia Espaciais, INPE, Cachoeira Paulista, Dez 2005.

Castro, A., Costa, F.S., Temperature Evolution and Propagation of Drying, Pyrolysis and Charring Fronts Inside Wood Slabs and Cylinders, 19th International Congress of Mechanical Engineering, COBEM 2007, Brasília- DF, Brasil, 2007.

Ellio, P.J., Whiteley, R.H., A Cone Calorimeter Test for the Measurement of Fammability Properties of Insulated Wire, Polymer Degradation and Stability, v. 64, p. 577-584, 1999.

Howell, J.P., Heat transfer, Boston, 665 p., 9. ed., MA : McGraw-Hill, c2002.

Howell, J.R., A Catalog Radiation Configuration Factors, McGraw-Hill Book Company, New York, 1982.

Hostikka, S. & Axelsson, J., Modelling of the radiative feedback from the flames in cone calorimeter. Espoo 2003. Nordtest, NT Techn Report 540. 41 p. NT Project 1575-02.

Janowska, G., Rybinski, P., Jantas, R., Effect of the Modification of Silica Properties and Flammability of Cross-Butadiene-Acrylonitrile Rubbers, Journal of Thermal Analysis and Calorimetry, v. 87, n.2, p. 511-517, 2007.

Price, D., Bullet, K.J., Cone calorimetry Studies of Polymer Systems Flame Retarded by Chemically Bwhered Phosphorus, Polymer Degradation and Stability, v. 88, p. 74-79, 2005.

Rea, S.N., Rapid Method for Determining Concentric Cylinder Radiation View Factors, AIAA J., vol 13, n.8, pp. 1122-1123, 1975.

Siegel, R., Howell, J. R., Thermal Radiation Heat Transfer, Taylor & Francis, USA, 3 rd, 1992.

## 8. RESPONSIBILITY NOTICE

The authors are the only responsible for the printed material included in this paper.